Nanoporous Melamine−Formaldehyde Gels by Microemulsion Templating

C. du Fresne von Hohenesche,* D. F. Schmidt, and V. Schädler

Received June 6, 2008. Revised Manuscript Received July 9, 2008

The polycondensation behavior of water-soluble melamine formaldehyde (MF) resins under acidic polymerization conditions was studied within a bicontinuous microemulsion comprising an oil phase (an alkane), a water phase (containing the reactive resin), and surfactant. The intrinsic nanoscopic feature size of such microemulsions was used as a structural template. Nonionic surfactants were found to be highly compatible with MF resin chemistry. Polycondensation using unmodified MF resins lead to gels showing large spherical voids arising from the separation of the oil phase. In contrast, by incorporating hydrophobic monomers such as benzoguanamine and caprinoguanamine into the resin (amphiphilic resin approach), a gel was formed consisting of aggregated nanoparticles confined within a continuous pore network. In this way, the effects of phase separation were successfully diminished, and porosities of 86 vol % ($\rho = 240$ g/L) were achieved with 65 nm pore sizes. Characterization of the materials was performed via scanning electron microscopy, nitrogen sorption at 77 K, and mercury intrusion.

Introduction

Nanoporous solids have attracted attention because of their optical, dielectric, and mass and heat transport properties.[1−7] A number of strategies have been developed for controlling the size, shape, and connectivity of the pore systems of these materials. Many of these strategies rely upon replicating nanostructures formed by surfactant phases using silica precursors, presumably through the intermediacy of a silicate−surfactant liquid crystal phase. The Mobil Oil group reported the best-known examples, namely MCM-41, MCM-48, and MCM-50, which are analogues of hexagonal *p6mm*, cubic *Ia3d* and lamellar liquid crystal phases, respectively.[8,9] Upon addition of a water-insoluble phase and adjusting the surfactant type and concentration, long-range-ordered lyotropic phases or microemulsions can also be obtained.

Microemulsions are macroscopically homogeneous, optically isotropic and two-phase mixtures of immiscible liquids, with surfactants giving a thermodynamically stable microstructure. The exact nature of this microstructure depends on the organization of the surfactant film separating the water and oil domains, which typically have dimensions of 10−500 nm.[10] The study of microemulsions with respect to surfactant efficiency, phase behavior, microstructure and dimensions, is of growing interest in both industry and academia.[11] These are promising systems for the production of nanostructured materials with novel properties for a variety of applications.[12] The objective of this study was to use aqueous polycondensation chemistry in combination with a structure-directing microemulsion template in order to obtain materials comparable to aerogels in terms of pore structure and porosity.

Aerogels are a special class of open-cell porous bodies derived from highly cross-linked inorganic or organic gels that are dried using special techniques to preserve a highly porous structure.[13] By definition, these materials are prepared through the sol−gel process and can be either granular or monolithic. Aerogels have ultrafine pore sizes (usually less than 100 nm), continuous porosity, high specific surface area, and a microstructure composed of interconnected colloid-like particles or polymeric chains with characteristic diameters. This microstructure is responsible for the unusual optical, acoustical, thermal, and mechanical properties of aerogels. Kistler prepared the first silica aerogels in the 1930s;[14] more recently, the aerogel concept has been applied to organic monomers/resins, expanding the range of achievable aerogel types and properties. These include melamine-formaldehyde (MF) aerogels,[15,16] resorcinol-formaldehyde (RF) aerogels,[17] phenolic-furfural (PF) aerogels,[18] and polyurethane aerogels.[19]

* Corresponding author. E-mail: cedric.duFresne@basf.com.

(1) Tejedor-Tejedor, M. I.; Vichi, F. M.; Anderson, M. A. *J. Porous Mater.* **2005**, *12* (3), 112.
(2) Adiga, S. P.; Brenner, D. W. *Nano Lett.* **2005**, *5* (12), 2509–2514.
(3) Silverstein, M. S.; Shach-Caplan, M.; Bauer, B. J.; Hedden, R. C.; Lee, H.; Landes, B. G. *Macromolecules* **2005**, *38* (10), 4301–4310.
(4) Jahromi, S. PCT Int. Appl. 2004, WO 2004-NL242 20040409.
(5) Fesmire, J. E. *Cryogenics* **2006**, *46* (3), 111–117.
(6) Reim, M.; Koerner, W.; Manara, J.; Korder, S.; Arduini-Schuster, M.; Ebert, H.-P.; Fricke, J. *Solar Energy* **2005**, *79* (2), 131–139.
(7) Matsuo, Y.; Ishibe, Y.; Kimura, K.; Nomura, K. Eur. Pat. Appl. 2006, EP 2005−255966 20050926.
(8) Kresge, C. T.; Leonowicz, M. E.; Roth, W. J.; Vartuli, J. C.; Beck, J. S. *Nature* **1992**, *359*, 710.
(9) Beck, J. S.; Vartuli, J. C.; Roth, W. J.; Leonowicz, M. E.; Kresge, C. T.; Schmitt, K. D.; Chu, C. T.-W.; Olson, D. H.; Sheppard, E. W.; McCullen, S. B.; Higgins, J. B.; Schlenker, J. L. *J. Am. Chem. Soc.* **1992**, *114*, 10834.
(10) Silas, J. A.; Kaler, E. W. *J. Colloid Interface Sci.* **2001**, *243*, 248.
(11) Sottmann, T. *Curr. Opin. Colloid Interface Sci.* **2002**, *7*, 5765.
(12) Hentze, H.-P.; Kaler, E. W. *Curr. Opin. Colloid Interface Sci.* **2003**, *8*, 164.
(13) Hüsing, N.; Schubert, U. *Angew. Chem., Int. Ed.* **1998**, *37*, 22–45.
(14) Kistler, S. S. *Nature* **1931**, *127*, 741.
(15) Pekala, R. W.; Alviso, C. T.; Kong, F. M.; Hulsey, S. S. *J. Non-Cryst. Solids* **1992**, *145*, 90.
(16) Pekala, R. W.; Alviso, C. T. *Mater. Res. Soc. Symp. Proc.* **1990**, *180*, 791.

10.1021/cm8015319 CCC: $40.75
Published on Web 09/19/2008

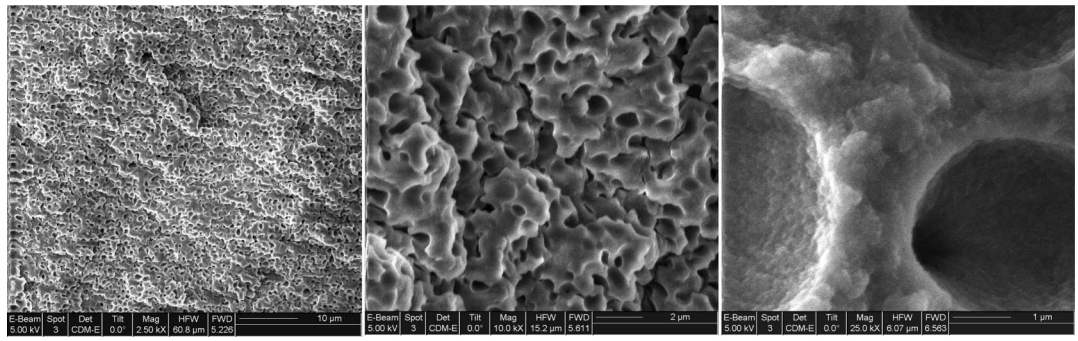

Figure 1. SEM micrographs of "MF1" microemulsion gel with increasing magnification from left to right. Reaction parameters: $T = 64.0$ °C, 8.3% *iso*-C_{13}-$(EO)_7$, 16.7% resin (M:F = 1:3.6); heptane volume fraction = 0.5; 4.3% H_3PO_4 in aqueous phase.

Table 1. Pore Structural Data of MF Microemulsion Xerogels

	nitrogen sorption				mercury intrusion				
sample	surface area (m^2/g)	pore volume (mL/g)	porediameter (nm)	porosity (%)	surface area (m^2/g)	pore volume (mL/g)	pore diameter (μm)	porosity (%)	density (kg/m^3)
MF1[a]					16.7	0.54	1.17	47.5	881
C9-MF1	289	1.6	55.0	72.7	162	2.3	0.36	79.5	345
C9-MF2	211	2.1	55.3	77.5	190	2.9	0.36	83.3	281
C9-MF3	360	2.5	64.6	80.6	189	3.6	0.47	85.8	239
Bzl-MF1[a]					165	2.32	0.26	79.6	343
Bzl-MF2[a]					179	3.11	0.47	83.9	270
Bzl-MF3[a]					154	3.37	0.66	85.0	253
Bzl-MF4	331	1.5	71.5	71.9	99	1.47	0.14	71.2	484

[a] Nitrogen sorption was not performed.

Table 2. Synthesis Parameters of MF Microemulsion Gels

sample	heptane/g	water/g	MF solution/g	surfactant/g (%)	acid/g (% in water phase)	Solids in water phase (%)	oil:water volume ratio
MF1	5.40	0	7.50	1.20 (8.3)	0.40 (4.3)	16.7	0.50
C9-MF1	5.40	0	7.50	1.20 (8.4)	0.25 (2.7)	12.7	0.50
C9-MF2	5.40	0	7.50	1.20 (8.3)	0.36 (3.9)	12.5	0.50
C9-MF3	5.40	0	7.50	1.20 (8.3)	0.40 (4.3)	12.4	0.50
Bzl-MF1	4.40	1.50	4.50	1.00 (8.5)	0.40 (5.3)	10.2	0.50
Bzl-MF2	4.75	1.50	4.50	1.00 (8.2)	0.40 (5.3)	10.2	0.52
Bzl-MF3	5.00	1.50	4.50	1.00 (8.1)	0.40 (5.3)	10.2	0.53
Bzl-MF4	4.40	2.50	3.50	1.00 (8.5)	0.30 (4.0)	8.1	0.50

Melamine formaldehyde (MF) condensation products belong to the class of amino resins or amino plastics and are closely related to their phenolic analogs both in synthesis and application.[20] Like urea (with a functionality $f = 4$), melamine ($f = 6$) reacts with formaldehyde under basic and acidic conditions to give a melamine-formaldehyde (MF) resin.[21] Polymerization of MF yields various methylolmelamines as well as a mixture of higher oligomers, with additional reaction giving rise to the formation of a network structure and eventually producing a rigid, high-T_g thermoset. The relative amounts of the various components are dependent on the reaction conditions (pH, catalyst, and resin stoichiometry). The cross-linking reaction involves the formation of both methylene-ether and methylene bridges.[22] The present work aims at combining the features of an organic aerogel-like structure with the mesostructure of a microemulsion template by utilizing aqueous melamine resins of different functionalities.

Results and Discussion

First, the structure- and size-directing capabilities of a bicontinuous microemulsion (free of excess oil or water phases) were applied to the aqueous-phase gelation of an MF resin containing melamine and formaldehyde at a molar ratio of 1:3.6. To select a bicontinuous microemulsion system, water/heptane/surfactant mixtures (using an *iso*-C_{13}-$(EO)_7$ type nonionic surfactant, HLB value = 12.5) were prepared at different ratios and their phase behavior was analyzed as a function of temperature.[23−25] Once the bicontinuous composition and temperature windows were identified, the water phase was substituted for an aqueous MF system and gelled under phosphoric acid catalysis. The SEM of a typical sample (MF1) after acid catalyzed polycondensation, removal of the template by solvent exchange and ambient drying is shown in Figure 1.

(17) Pekala, R. W. *J. Mater. Sci.* **1989**, *24*, 3221.
(18) Pekala, R. W.; Alviso, C. T.; Lu, X.; Gross, J.; Fricke, J. *J. Non-Cryst. Solids* **1995**, *188*, 34–40.
(19) Biesmans, G.; Mertens, A.; Duffours, L.; Woigner, T.; Phalippou, J. *J. Non-Cryst. Solids* **1998**, *225*, 64.
(20) Odian, G. *Principles of Polymerization*; John Wiley & Sons: New York, 1991; pp 132−134.
(21) Nair, R.; Francis, D. J. *Polymer* **1983**, *24*, 626.
(22) Jones, F. N.; Chu, G.; Samaraweera, U. *Prog. Org. Coat.* **1999**, *24*, 189–208.
(23) Kahlweit, M.; Strey, R.; Firman, P. *J. Phys. Chem.* **1986**, *90*, 671–677.
(24) Burauer, St.; Sachert, Th.; Sottmann, Th.; Strey, R. *Phys. Chem. Chem. Phys.* **1999**, *1*, 4299–4306.
(25) Kahlweit, M.; Strey, R.; Firman, P.; Haase, D.; Jen, J.; Schomäcker, R. *Langmuir* **1988**, *4*, 499.

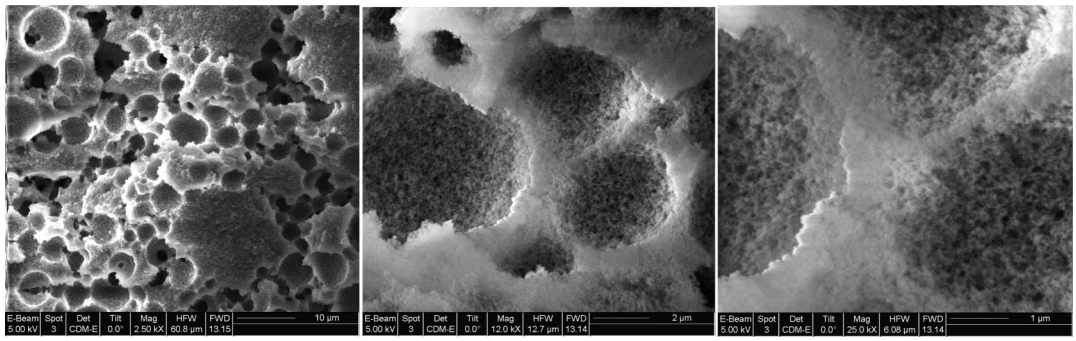

Figure 2. SEM micrographs of "C9-MF1" microemulsion gel with increasing magnification from left to right. Reaction Parameters: $T = 60.0$ °C, 8.4% *iso*-C_{13}-$(EO)_7$, 12.7% resin (90 mol % melamine, 10 mol % caprinoguanamine, M:F = 1:3.6), heptane volume fraction = 0.5, 2.7% H_3PO_4 in aqueous phase.

Microemulsion gels produced in this fashion shrank heavily upon subcritical drying. The translucent solid possessed micrometer-sized holes, suggesting phase separation of discrete oil droplets (i.e., through the polymerization-induced formation of an oil-in-water emulsion) and a coarsening of the structure. This is consistent with reports of translucency in microemulsion-templated gels with micrometer-sized pores.[26,27] Likewise, this supports the generality of the demixing phenomena reported to occur in similar systems during polymerization.[28,29] Although the large pores are homogeneously distributed in the solid, the pore morphology is discontinuous. Mercury intrusion revealed the largest pore volume for 1.1 μm sized pores and detected a small amount of wall porosity with a pore size on the order of 20 nm (see Table 1).

The phase separation observed most likely occurs as a consequence of incompatibility of the polymerizing species with the bicontinuous microemulsion.[28,29] To prevent this, we focused on making the polymer itself more surface-active - similar to the use of surfmers in the successful reproduction of similar surfactant mesophases.[30] To accomplish this, we partially substituted melamine (2,4,6-triamino-1,3,5-triazine) by 2,4-diamino-6-nonyl-1,3,5-triazine, aka caprinoguanamine (C9-MF gels), and 2,4-diamino-6-phenyl-1,3,5-triazine, aka benzoguanamine (Bzl-MF gels), in the synthesis under otherwise similar reaction conditions.

Three caprinoguanamine-containing MF gels (C9-MF1 to C9-MF3, 10 mol % substitution of melamine by caprinoguanamine) were produced via microemulsion templating using the *iso*-C_{13}-$(EO)_7$ nonionic surfactant and heptane under phosphoric acid catalysis. The amount of acid (catalyst) was increased from 2.7 wt % (C9-MF1) to 3.9 wt % (C9-MF2) and to 4.3 (C9-MF3) (see Table 2). The microemulsion gel morphology was, to our surprise, similar to the unmodified MF cases: Heptane droplets had phase-separated and were interspersed within a continuous gel phase. SEM investigations (see Figure 2), however, revealed significant wall porosity not previously observed: Higher-magnification SEM micrographs clearly show pores in the range between 50 and 200 nm. Such hierarchical pore structures resemble those reported by Antonietti et al. following critical point drying.[28] The disappearance of the bicontinuous microemulsion structure along with the production of a variety of pore structures supports the idea of kinetically controlled structuration involving multiple phase transitions potentially coupled with the nucleation and growth of domains within preorganized media.[28,29] Mercury intrusion and nitrogen sorption were performed in order to quantify porosity and pore size distributions (PSDs) of the C9-MF microemulsion gels. These two methods gave initially contradictory results that were found to be typical for highly nanoporous solids.[31]

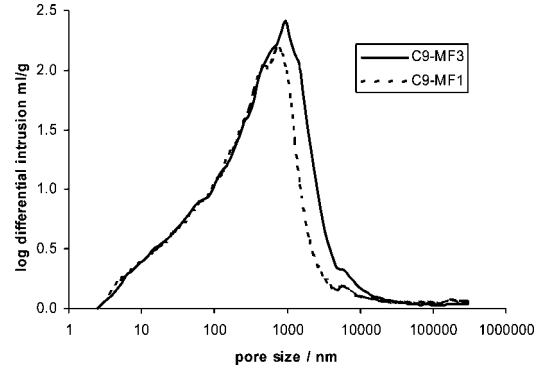

Figure 3. Pore size distribution (PSD) curves of C9-MF samples from mercury intrusion.

Mercury intrusion porosimetry (see Figure 3) detected pore sizes from 10 μm down to 3.7 nm (lower detection limit), in stark contrast to the nitrogen sorption results (see Figure 4), which indicated a monomodal PSD with a sharp peak in the range of 40−80 nm.

Although SEM micrographs confirmed the presence of large pores, it was clear from these results that the continuous PSDs obtained via mercury intrusion (Figure 3) were not accurate representations of the structure of the pore network. In fact, these data are excellent examples of the so-called "damage curve".[32,33] This response is observed in highly

(26) Yan, F.; Texter, J. *Angew. Chem., Int. Ed.* **2007**, *46*, 2440–2443.
(27) Yan, F.; England, D.; Gu, H.; Texter, J. *Polym. Mater. Sci. Eng.* **2007**, *97*, 534–355.
(28) Antonietti, M.; Caruso, R. A.; Göltner, Ch. G.; Weissenberger, M. C. *Macromolecules* **1999**, *32*, 1383–1389.
(29) Hentze, H.-P.; Antonietti, M. *Curr. Opin. Solids State Mater. Sci.* **2001**, *5*, 343.
(30) Yan, F.; Texter, J. *Adv. Colloid Interface Sci.* **2006**, *128−130*, 27–35.
(31) Egger, C. C.; du Fresne, C.; Raman, V. I.; Schädler, V.; Frechen, T.; Roth, S. V.; Müller-Buschmann, P. *Langmuir* **2008**, *24*, 5877–5887.
(32) Scherer, G. W.; Smith, D. M.; Stein, D. *J. Non-Cryst. Solids* **1995**, *186*, 309–315.
(33) Scherer, G. W.; Smith, D. M.; Qiu, X.; Anderson, J. *J. Non-Cryst. Solids* **1995**, *186*, 316–320.

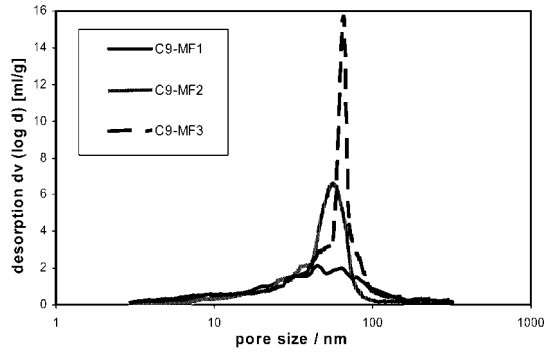

Figure 4. Pore size distribution (PSD) curves of C9-MF samples from nitrogen sorption.

nanoporous solids in particular because the pressures needed to crush these solids are less than those required for mercury intrusion. As a result of the crushing of these samples, "intruded volume" was detected by the apparatus, with the PSDs produced reflecting not pore structure but mechanical stability under hydrostatic compression. Regardless of whether the pores are crushed or intruded, however, the total porosity is always correctly assessed. Nitrogen sorption on the other hand is limited by an upper pore size limit (∼150 nm) but gives reliable results for mesopore size distributions. As such, throughout this report we refer to the total porosity as measured by mercury intrusion, but sometimes favor the BJH desorption[34] pore size from gas sorption over the volume median intrusion pore size from mercury intrusion when it is obvious that the latter technique has crushed the sample.

Increasing amounts of phosphoric acid (catalyst) clearly lead to shorter gel times, which resulted in the structural fixation at an earlier stage of the nucleation and growth reaction, indicating the strong kinetic control of the observed structure formation. As a result, the number of pores with dimensions of 55−65 nm increased significantly, resulting in a significant increase in total porosity as well. A comparison of the data obtained from mercury intrusion and nitrogen sorption again reveals distinct differences (see Table 1). Nitrogen sorption is more useful in characterizing the mesopore size distribution; however, the full porosity cannot be assessed because of the known method-related restrictions. Data from the C9-MF samples clearly emphasize the necessity of combining and carefully evaluating several analytical methods in order to form an accurate picture of the pore structures of this class of porous solids.

Analogous to the previous work with caprinoguanamine-modified MF, benzoguanamine-modified MF gels were also prepared (Bzl-MF). Again, a 10 mol % substitution of melamine was used in the synthesis, and the volumetric ratio of water to heptane in the microemulsion template was varied from 0.50 (Bzl-MF1) to 0.52 (Bzl-MF2) to 0.53 (Bzl-MF3). As expected, the increase of the heptane phase was generally accompanied by higher porosity (see Table 1). In the case of Bzl-MF4, a system with a lower MF solids content in the aqueous phase, SEM micrographs (Figure 5) show complete suppression of phase separation, allowing for effectively all of the pores to be detected via nitrogen sorption. The cocontinuous pore morphology can be seen in these micrographs as well (Figure 5, right). The nanostructure of the gels thus produced comprises MF nanoparticles with sizes between 20 and 50 nm.

As before, mercury intrusion shows the typical damage curve (Figure 6), with nitrogen sorption offering more reliable results. Hysteresis between the adsorption and desorption branch was observed (Figure 7), giving additional information on the pore network: The PSDs calculated from the branches differ in the location of their peak maxima, indicating heterogeneities within the pores. In other words, the pores cannot be perfectly cylindrical in shape, as confirmed by SEM. The common practice of deducing the average pore size from the desorption branch was therefore applied here, as the mechanism of nitrogen desorption is theoretically well described by the BJH method. The pore structure data for various Bzl-MF microemulsion gels are summarized in Table 1. Materials densities vary between 253 and 484 g/L, with higher porosity correlated with larger pores and vice versa. The Bzl-MF gels therefore represent promising candidates for producing aerogel-like structures via microemulsion templating. However, detailed analysis of the PSDs was only possible in the sample with the smallest pores (Bzl-MF4) because of the aforementioned problems related to the high pressures applied in mercury intrusion porosimetry.

Summary

The polycondensation behavior of melamine formaldehyde (MF) resins under acidic polymerization conditions has been studied within a bicontinuous microemulsion comprising an oil phase (heptane), a water phase (containing a reactive resin), and an *iso*-C_{13}-$(EO)_7$ type nonionic surfactant. Pure MF resins lead to gels showing phase separation of the oil phase. By incorporating alkyl and phenyl groups into the resin, gels were formed consisting of a continuous aggregated nanoparticle phase with a continuous pore network. Thus, macroscale phase separation was successfully suppressed and porosities between 80 and 85 vol% were achieved with 65−400 nm pore sizes. The suppression of macroscale phase separation by increasing the compatibility of the formed polymer matrix with the template structure (which is strongly related to attractive and repulsive interactions at interfaces, and where enthalpic and entropic effects play a key role) was only one requirement. The second requirement was to kinetically trap the structure of the mesophase via a rapid reaction process. With that said, it is clear from these results that true replication of the original mesophase structure is a complex matter, given that the mesophase is by no means static during this process, even when the polycondensation chemistry is relatively rapid. In particular, multiple phase transitions during polymerization within the organized media are most likely coupled with domain nucleation and growth, leading to hierarchically structured materials with morphologies and length scales that differ significantly from the original microemulsion structure. The characterization efforts reported here reveal that highly porous solids produced by this method and containing pores smaller than 500 nm must be carefully analyzed from a structural point of view because

(34) Barrett, E. P.; Joyner, L. E.; Halenda, P. P. *J. Am. Chem. Soc.* **1951**, *73*, 373.

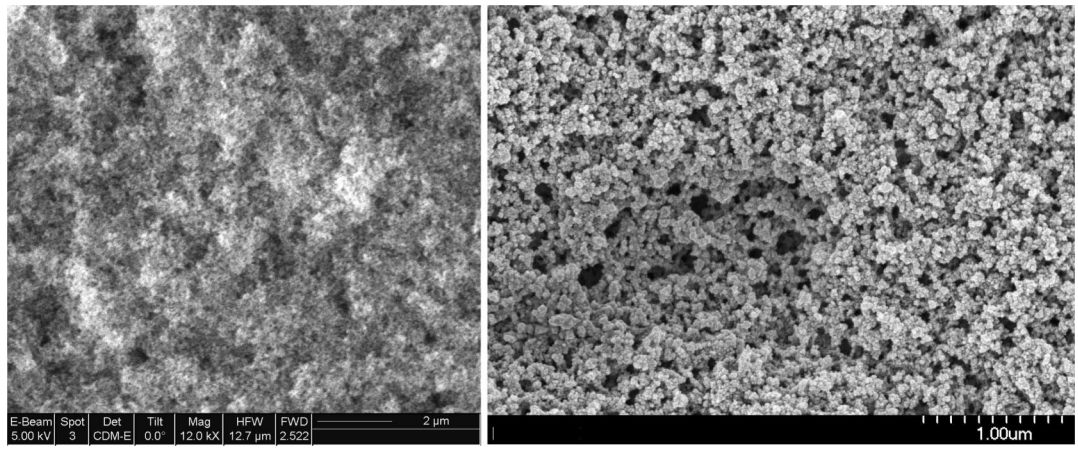

Figure 5. SEM micrographs of "Bzl-MF4" microemulsion gel with increasing magnification from left to right. Reaction parameters: $T = 60.0$ °C, 8.5% *iso*-C_{13}-$(EO)_7$, 8.1% resin (90 mol % melamine, 10 mol % benzoguanamine, M:F = 1:3.6), heptane volume fraction = 0.5, 4.0% H_3PO_4 in aqueous phase.

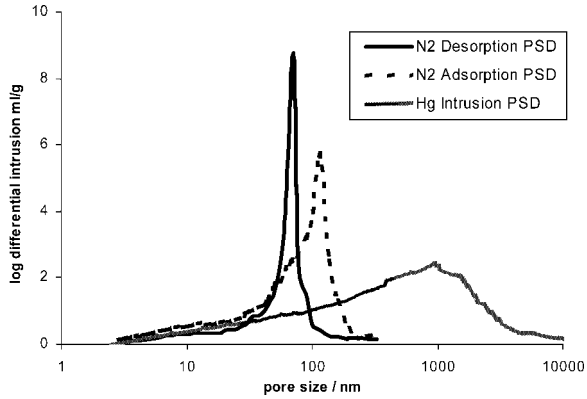

Figure 6. PSD curves of Bzl-MF4 from nitrogen sorption (adsorption and desorption branch) and from mercury porosimetry.

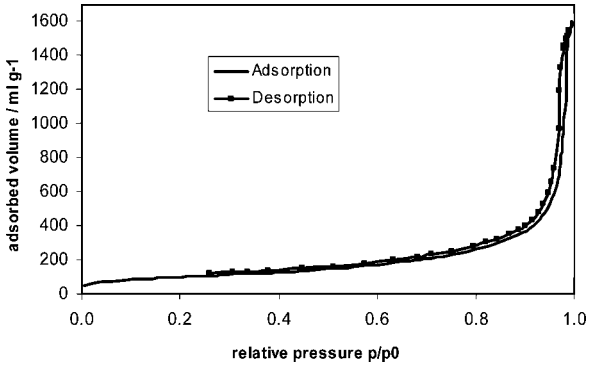

Figure 7. Nitrogen sorption isotherm of Bzl-MF4.

of the limitations of existing analytical methods. In most cases, only a combination of SEM, nitrogen sorption, and mercury intrusion gives satisfactory results.

Experimental Section

Synthesis of Melamine Formaldehyde Solution "MF Solution". In a 1 L three-necked round-bottom flask equipped with a magnetic stir bar, 300 mL of deionized water and 115.8 g of formaldehyde solution (37 wt %, Sigma Aldrich) were added under stirring. The pH was increased by adding 0.82 g solid sodium hydroxide (pH 9.6), after which 50.0 g melamine (purum, Fluka) was added. The flask containing the resultant milky dispersion was then immersed in a preheated (80 °C) silicone oil bath. As the reaction product of formaldehyde with melamine has greater water-solubility than melamine alone, the dispersion was transformed into a clear solution after 18 min ($T_{reaction} = 68$ °C), and became clear solution after 22 min ($T_{reaction} = 70$ °C). The solution was maintained at its final temperature for 10 min, then cooled to room temperature and filtered to remove any insoluble matter. The solids content (as measured using a moisture balance) amounted to 17.6% by weight.

Synthesis of Melamine/Caprinoguanamine Formaldehyde Solution "C9-MF Solution". In a 1 L, three-necked round-bottom flask equipped with a magnetic stir bar, 400 mL of deionized water and 115.6 g of formaldehyde solution (37 wt %, Sigma Aldrich) were added under stirring. The pH was increased by adding 0.78 g of solid sodium hydroxide (pH 9.5); 39.11 g of melamine (purum, Fluka) and 10.02 g of 2,4-diamino-6-nonyl-1,3,5-triazine (>97%, Degussa) were then added, and the flask containing the resultant milky dispersion was immersed in a preheated (120 °C) silicone oil bath. $T_{reaction}$ reached 70 °C after 15 min, 79 °C after 25 min, and 92 °C after 40 min; the reaction was stopped after one hour ($T_{reaction} = 97$ °C). The milky solution was cooled to room temperature, but was not filtered based on the observation that clarity was never achieved during the resin synthesis, indicating poor water solubility of the resin, presumably due to the presence of its long alkyl substituents. The solids content (as measured using a moisture balance) amounted to 13.1%.

Synthesis of Melamine/Benzoguanamine Formaldehyde Solution "Bzl-MF Solution". In a 1 L, three-necked round-bottom flask equipped with a magnetic stir bar, 400 mL of deionized water and 117.5 g of formaldehyde solution (37 wt.%, Sigma Aldrich) were added under stirring. The pH was increased by adding 0.78 g of solid sodium hydroxide (pH 9.7); 42.8 g of melamine (purum, Fluka) and 7.1 g of 2,4-diamino-6-phenyl-1,3,5-triazine (>98%, Degussa) were then added, and the flask containing the resultant milky dispersion was immersed in a preheated (80 °C) silicone oil bath. $T_{reaction}$ reached 63 °C after 10 min (with clarity observed after 12 min) and 68 °C after 30 min; the reaction was stopped after 40 min ($T_{reaction} = 69$ °C). The clear solution was cooled to room temperature and filtered to remove any insoluble matter. The solids content (as measured using a moisture balance) amounted to 14.5%.

Gelation in a Water/Heptane/*iso*-Tridecylheptaglycol Microemulsion. Microemulsion phase studies indicated a wholly bicontinuous structure with no excess oil or water phases at 62.5 °C with the following microemulsion composition: Heptane:water volume ratio = 0.5, surfactant total mass ratio = 0.085 (see Figure

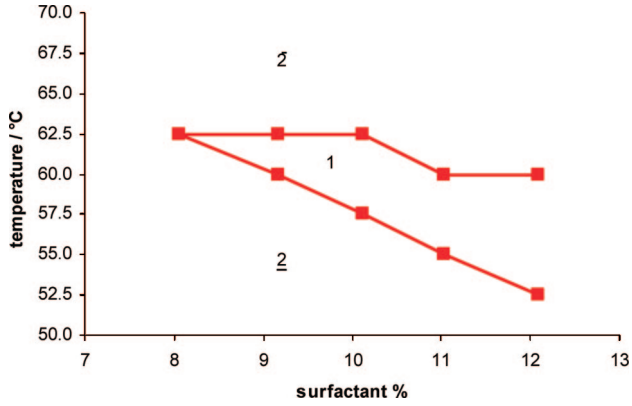

Figure 8. Binary phase diagram "fish diagram" of the studied oil−surfactant−water microemulsion, showing the evolution from a two-phase region toward a one-phase region with bicontinuous structure with increasing surfactant concentration or temperature.[35]

8). This system was used as starting point for the following gelation experiments.

Gelation of MF Solution. In the following sequence heptane (purum, Fluka), iso-tridecylheptaglycol, aka *iso*C_{13}-$(EO)_7$ (industrial grade, BASF SE), MF solution (17.6% nonvolatile components) and phosphoric acid solution (85%, Aldrich) were weighed into a glass test tube according to Table 2. The tube was capped and sealed, shaken, and immediately put into a thermostatted water bath at 64.0 °C (this slight shift being necessary to retain the desired bicontinuous structure because of the effects of the MF and acid on the phase behavior of the microemulsion). During the first 3 mi of heating, the tube was shaken several times, after which gelation was allowed to occur. The microemulsion completely gelled after 10 min as a white gel. Postreaction was allowed for further 12 h; the tube was then cooled and crushed, and the white monolith was solvent-exchanged twice with pentane (purum, Fluka) and dried at ambient conditions.

Gelation of C9-MF Solution. In the following sequence heptane (purum, Fluka), *iso*-C_{13}-$(EO)_7$ (industrial grade, BASF SE), C9-MF solution (13.1% nonvolatile components), and phosphoric acid solution (85%, Aldrich) were weighed into a glass test tube according to Table 2. The tube was capped and sealed, shaken and immediately put into a thermostatted water bath at 60.0 °C. During the first 3 min of heating, the tube was shaken several times, after which gelation was allowed to occur. The microemulsion was clear after 7 min, indicating no major changes in the equilibrium microemulsion structure, and turned bluish after 11 min, indicating reaction of the MF. The microemulsion became turbid after 15 min and was completely gelled after 25 min (white gel). Postreaction was allowed for further 12 h; the tube was then cooled and crushed and the white monolith was solvent-exchanged twice with pentane (purum, Fluka) and dried at ambient conditions.

Gelation of Bzl-MF Solution. In the following sequence heptane (purum, Fluka), iso-tridecylheptaglycol (industrial grade, BASF SE), Bzl-MF solution (14.5% nonvolatile components), water and phosphoric acid solution (85%, Aldrich) were weighed into a glass test tube according to Table 2. The tube was shaken and immediately put into a thermostatted water bath at 60.0 °C. During the first 3 min of heating, the tube was shaken several times, after which gelation was allowed to occur. The microemulsion was clear after 4 min, indicating no major changes in the equilibrium microemulsion structure, and turned bluish after 9 min, indicating reaction of the MF. The microemulsion became turbid after 13 min and was completely gelled after 20 min (white gel). Postreaction was allowed for further 12 h; the tube was then cooled and crushed and the white monolith was solvent-exchanged twice with pentane (purum, Fluka) and dried at ambient conditions.

Analysis

A field-emission scanning electron microscope (FEI Dual Beam 235) was used in these studies. Sputtering with gold was a necessity for all polymeric materials.

Nitrogen sorption measurements were performed on a Quantachrome Autosorb 6B (Quantachrome Corporation, Boynton Beach, FL) automatic adsorption instrument. Before measurements, 100−150 mg of the samples was heated at 60 °C under a high vacuum (1×10^{-5} Pa) for at least 12 h. Specific surface areas were calculated according to the BET equation,[36] the specific pore volume according to Gurwitsch[37] and the average pore diameter according to the BJH method.

Mercury intrusion was performed using a Micromeritics Autopore IV mercury intrusion porosimeter. Samples were outgassed for 30 min at 0.08 mbar prior to measurements.

CM8015319

(35) Kahlweit, M.; Strey, R. *Angew. Chem., Int. Ed.* **1985**, *24*, 654–668.
(36) Brunauer, S.; Emmet, P. H.; Teller, E. *J. Am. Chem. Soc.* **1938**, *60*, 309.
(37) Gurwitsch, L. G. *J. Phys. Chem. Soc. Russ.* **1915**, *47*, 805.